

Low-profile Hybrid-mode Antenna Providing Near-hemispherical Field-of-view Coverage

Ren Wang, Bing-Zhong Wang, Xiao Ding, and Changhai Hu

Institute of Applied Physics

University of Electronic Science and Technology of China, Chengdu, 610054, China

rwang.uestc@hotmail.com, bzwang@uestc.edu.cn, xding@uestc.edu.cn

Abstract — The hybrid-mode model (HMM) combining monopole and dipole radiation modes can provide near-hemispherical coverage but has a high profile. To reduce the profile of HMM, a modified HMM is presented in this paper using a dipole radiator and a magnetic current loop radiator. Based on the modified model, a low-profile on-board antenna is proposed. When the side length of the ground is infinite, the 3-dB beamwidths in the xz plane and yz plane of the proposed antenna are both 180° . When the side length of the ground is finite, the proposed antenna can provide a near-hemispherical field-of-view coverage. The design example demonstrates the practicability of the modified HMM and the proposed antenna can be used in wide-angle scanning arrays and rich-multipath communication systems.

Index Terms — Broad beam, hemispherical coverage, hybrid modes, low profile, wide-angle scanning.

I. INTRODUCTION

The hybrid-mode model (HMM) combining monopole radiation mode and dipole radiation mode is a traditional and popular method to obtain near-hemispherical field-of-view coverage [1], [2]. The dipole model and monopole mode can provide horizontally polarized patterns and vertically polarized patterns [3]-[5], respectively. The peaks and nulls of the HMM can be controlled by adjusting the monopole height and dipole length. Therefore, the HMM is possible to achieve a near hemispherical field-of-view coverage [1], [2]. Recently, the hemispherical coverage was also obtained using half-loop antennas [6], [7], which can be considered as the transformation of HMM.

In wide-angle scanning arrays, the HMM has been used to design broad-beam elements. In [8], [9], two parasitic monopoles with reactive loads were placed near a driving dipole to broaden the E-plane pattern of dipole antennas. In [10]-[12], the dipole-mode radiator surrounded by monopoles was used to achieve near-hemispherical coverage for wide-angle scanning phased arrays. In wireless communication systems, a single antenna with dipole radiation mode and monopole

radiation mode can provide antenna diversity and improve system reliability in rich multipath environments [13], [14]. In radio astronomy systems (RAS), the HMM with near-hemispherical field-of-view coverage and polarization discrimination capability is particularly important [15], [16]. To use HMM antenna in RAS, a theoretical sensitivity analysis of HMM antennas was proposed in [17] and [18]. In addition, the HMM has been used to simplify hemispherical two-dimensional angular space null steering [19].

Although the HMM has been extensively investigated and widely used in several applications, the high profile of monopole radiator is an existing problem to this model and the mentioned HMM antennas have a profile of approximately $\lambda/4$, where λ is the wavelength corresponding to center operation frequency. To reduce the profile, the HMM is modified in this paper by using a dipole radiator and a magnetic current loop (MCL) radiator. The radiation patterns of MCL and dipole can cover the low elevation area and high elevation area, respectively. Therefore, a near-hemispherical coverage can be obtained by optimizing the weights of the two radiation modes. Based on the modified hybrid-mode model (MHMM), a low-profile on-board antenna with near-hemispherical field-of-view coverage is proposed. When the side length of the ground is infinite, the 3-dB beamwidths in the xz plane and yz plane of the proposed hybrid-mode antenna are both 180° . The design example demonstrates the practicability of the MHMM and the proposed antenna can be used in wide-angle scanning arrays and radio astronomy systems.

II. LOW-PROFILE ANTENNA WITH NEAR-HEMISPHERICAL COVERAGE

A. Low-profile hybrid-mode model

To lower the profile of HMM, a substitute with a similar radiation pattern of monopole radiator should be found firstly. According to [20] and [21], MCL has a monopole-like radiation pattern. Therefore, the MCL is used to replace the monopole radiator in this paper. The radiation pattern of MCL is shown in Fig. 1. The models are simulated by CST Microwave Studio. Because CST

software has no magnetic currents, the MCL on an electric wall is represented with an electric current loop with a radius of $\lambda/40$ placed on an infinite magnetic wall in the simulation, i.e., the complementary structure of MCL. The distance between the loop and the magnetic wall is $\lambda/40$, where λ is the free-space wavelength. From Fig. 1, we can see that the pattern of MCL and that of monopole are very similar. Therefore, a low-profile MHMM with near-hemispherical pattern may be obtained if the MCL and dipole can be excited at the same time.

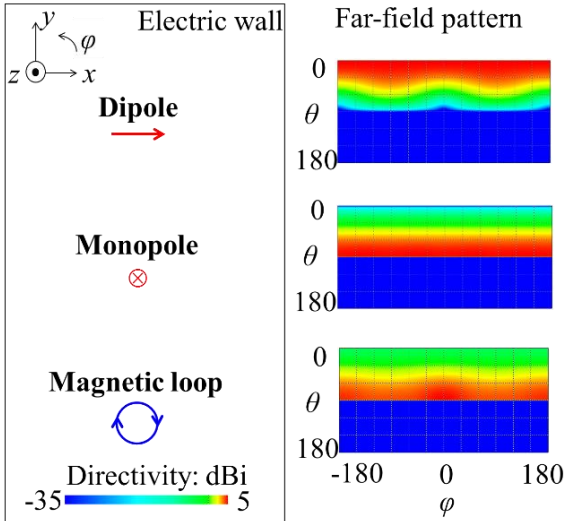


Fig. 1. Dipole, monopole, and magnetic current loop on an infinite electric wall and their radiation patterns. The models are simulated by CST Microwave Studio.

B. Antenna with near-hemispherical coverage

Based on the MHMM combining a dipole radiator and a MCL radiator, a microstrip on-board antenna at L band is proposed to provide a near-hemispherical pattern. Geometry of the proposed antenna is shown in Fig. 2 and its optimum dimensions are marked in the figure. This antenna is composed of two kinds of dielectric substrates and three layers of copper patches. The top substrate has a thickness of 4 mm and a relative dielectric constant of 2.65; the bottom substrate has a thickness of 1.6 mm and a relative dielectric constant of 4.4. A narrow rectangular patch and a circular patch are printed on the top and bottom substrates. The narrow patch can provide a radiation similar to a dipole on an electric wall. The circular patch with opened edge is fed from the center and the electric field is from the patch to the ground, therefore, the edge of the circular patch can be equivalent to a MCL radiator. The two patches are connected with a copper via and fed from the backside with a 50- Ω coaxial probe. The whole dimension of the radiation patches is approximately $0.2\lambda \times 0.1\lambda \times 0.03\lambda$.

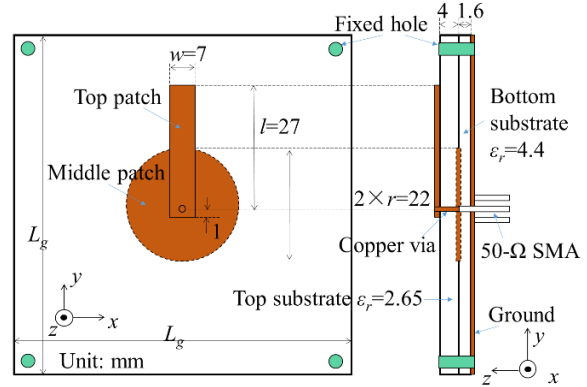


Fig. 2. Geometry of the hybrid-mode antenna. The color brown represents copper material. The dimensions are optimized by CST.

According to the boundary condition, the radiation pattern of MCL radiator, similar to monopole, can cover to the ground plane only when the ground is infinite. As a result, the HMM, as well as the MHMM, can potentially provide a hemispherical coverage only when the ground is infinite. To eliminate the effect of ground, the ground is set to be infinite when optimizing parameters. The simulated reflection coefficient of the proposed antenna with an infinite ground is shown in Fig. 3. The simulated band with S11 below -10 dB includes 1.6 GHz, which is the desired operating frequency.

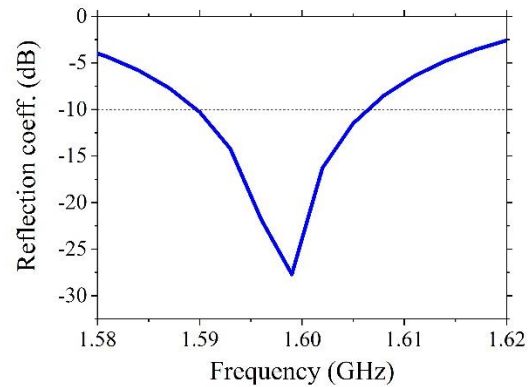


Fig. 3. Simulated reflection coefficient of the hybrid-mode antenna with an infinite ground.

For the hemispherical-pattern antenna, radiation on each direction should be equal. However, the exact condition is difficult to practically use in the numerical calculation. To simplify the hemispherical-pattern condition, a five-equal-points condition is used to optimize the radiation pattern. The five key control points of a hemispherical pattern are $(\theta=90^\circ, \varphi=90^\circ)$, $(\theta=90^\circ, \varphi=180^\circ)$, $(\theta=90^\circ, \varphi=270^\circ)$, $(\theta=90^\circ, \varphi=0^\circ)$, and

($\theta=0^\circ$), respectively. Because the five-equal-points condition is a necessary but not sufficient condition for the hemispherical pattern, the radiation pattern should be checked after optimization. The simulated radiation patterns at 1.6 GHz of the proposed antenna with an infinite ground are shown in Fig. 4. When the ground is infinite, the 3-dB beamwidths in the xz plane and yz plane are both 180° and the pattern fluctuation in the xy plane is less than 5 dB. In the design process, we consider a hemispherical pattern is obtained when the 3-dB beamwidths in both xz plane and yz plane are 180° .

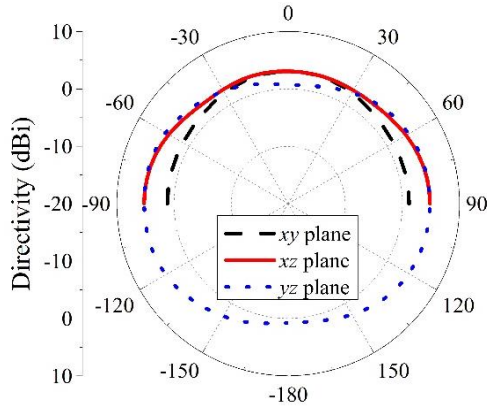


Fig. 4. Simulated patterns at 1.6 GHz of the hybrid-mode antenna with an infinite ground.

From the principle of the MHMM, the dipole can cover the high-elevation area and the MCL can cover the low-elevation area. A near-hemispherical coverage may be obtained only when the appropriate weight factors of the two kinds of radiations are satisfied. For the proposed hybrid-mode antenna, the weight factor can be adjusted by structure parameters. Next, the effect of the length l of the narrow rectangular patch is analyzed as an example, as shown in Fig. 5 and Fig. 6.

The simulated patterns at 1.6 GHz in the xz plane of the proposed hybrid-mode antenna corresponding to different length l are shown in Fig. 5. From these figures, we can see that the φ component can cover the high-elevation area and the θ component can cover the low-elevation area. The polarization discrimination capability is particularly important to rich multipath environments [13], [14]. When the length l increases, the radiation of φ component is strengthened and the radiation of θ component is weakened. When l is less than 27 mm, the radiation maximum of θ component is larger than φ component and the sum radiation pattern has a depression around 0° . When l is more than 27 mm, the radiation maximum of θ component is smaller than φ component and sum radiation pattern has a narrow broadside pattern. When $l=27$ mm, the two components have similar radiation maximums and a broad coverage of the sum radiation is obtained.

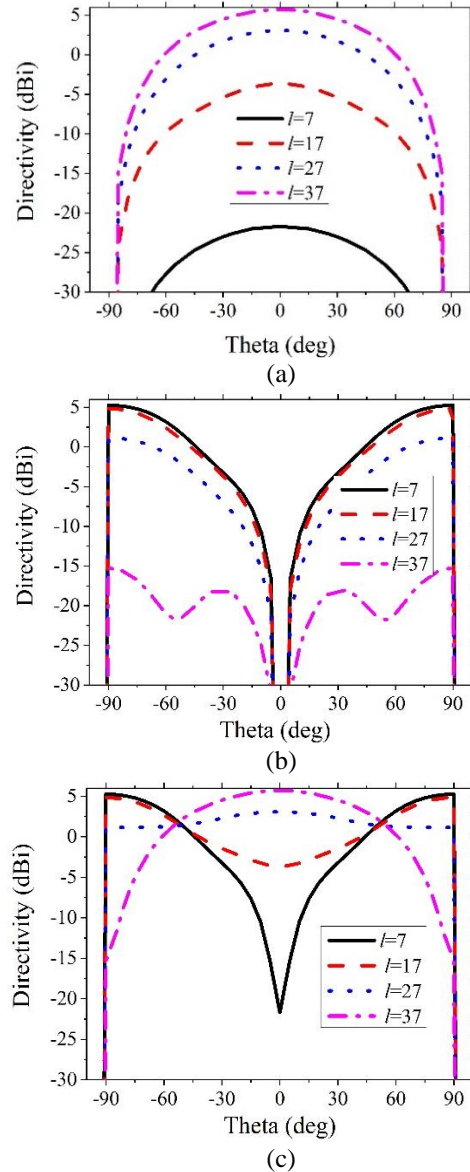


Fig. 5. Simulated patterns at 1.6 GHz in the xz plane corresponding to different length l of the narrow rectangular patch: (a) φ component, (b) θ component, and (c) vector sum of the two components. The unit of l is mm.

The simulated patterns at 1.6 GHz in the yz plane of the proposed hybrid-mode antenna corresponding to different length l are shown in Fig. 6. The radiation of θ component is much larger than φ component. The low cross polarization radiation in the yz plane of the MHMM antenna is similar to that of the monopole radiator in HMM, which indicates that the MCL will not cause cross polarization in the H-plane of dipoles [8], [9]. This phenomenon is appropriate for wide-angle scanning arrays. When $l=27$ mm, a 180° coverage of θ component is obtained. Therefore, the radiations of

the proposed antenna can be controlled by adjusting structure parameters to realize a near-hemispherical coverage.

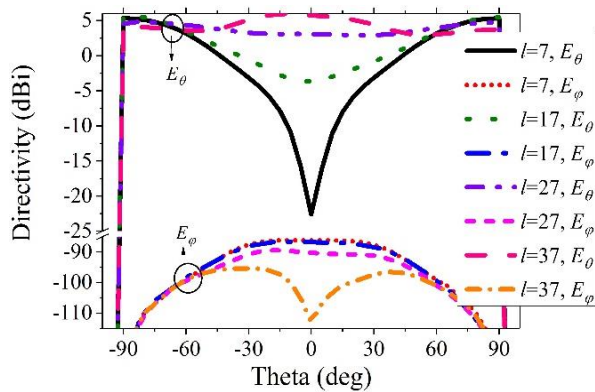


Fig. 6. Simulated patterns at 1.6 GHz in the yz plane corresponding to different length l of the narrow rectangular patch. The unit of l is mm.

The above discussions are under the circumstance of infinite ground. The performances of the proposed hybrid-mode antenna with finite ground are shown in the following. Two prototypes of the proposed antenna, with $L_g=\lambda$ and $L_g=4\lambda$ respectively, are fabricated. Two photographs of unassembled and assembled antenna with $L_g=\lambda$ are shown in Fig. 7.

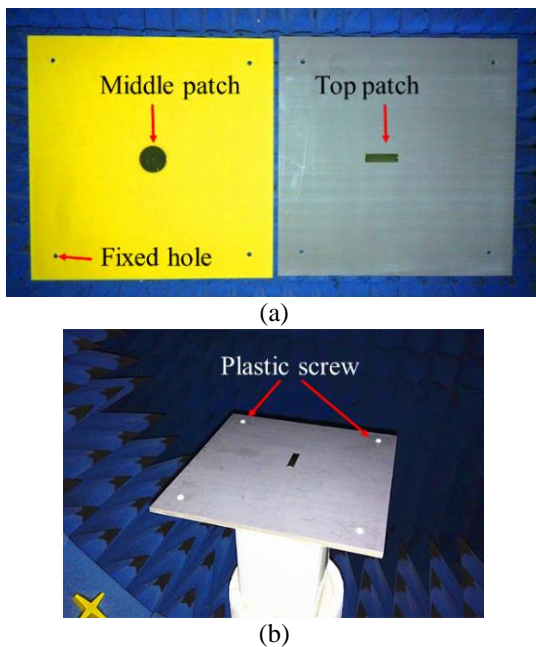


Fig. 7. Photographs of the hybrid-mode antenna with $L_g=\lambda$: (a) unassembled antenna and (b) assembled antenna.

The simulated and measured reflection coefficients of the proposed antenna are shown in Fig. 8. From Fig. 8, we can see that the resonant frequency changes little with L_g . The ground size has little effect on the resonant frequency in both simulated results and the measured results. The simulated and measured bands with S_{11} below -10 dB both include 1.6 GHz. The measured resonant frequency has a little move toward the high frequency because of the machining error, which includes the soldering error, the assembled error, and parameters error of practical substrate.

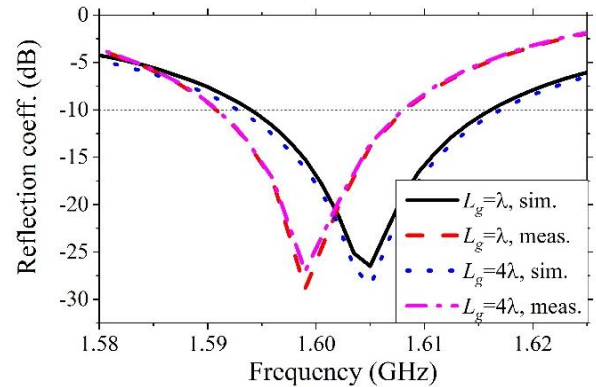


Fig. 8. Simulated and measured reflection coefficients of the hybrid-mode antenna when $L_g=\lambda$ and $L_g=4\lambda$. The resonant frequency changes little with L_g .

The far-field radiation pattern is measured in a microwave anechoic chamber. The simulated and measured radiation patterns of the proposed antenna with different L_g are shown in Fig. 9. When L_g is λ , the simulated 3-dB beamwidth in the xz plane is 128° and the measured one is 130° ; the simulated 3-dB beamwidth in the yz plane is 147° and the measured one is 140° . When $L_g=4\lambda$, the simulated 3-dB beamwidth in the xz plane is 152° and the measured one is 161° ; the simulated 3-dB beamwidth in the yz plane is 175° and the measured one is 172° . The 3-dB beamwidths in the xz plane and yz plane both increase with L_g . From the simulated and measured results, we can also see that when $L_g=4\lambda$, the side lobe level is significantly lower than that in the case of $L_g=\lambda$. The proposed antenna has a broad beam and can provide a near-hemispherical coverage with a finite ground.

The measured efficiencies and peak gains of the proposed antenna are shown in Fig. 10. When $L_g=\lambda$ and $L_g=4\lambda$, the measured efficiencies are both more than 60% in the frequency band of 1.59 GHz-1.62 GHz. The peak gain in the case of $L_g=\lambda$ is a little higher than that in the case of $L_g=4\lambda$ because the radiation beam is broader when $L_g=4\lambda$.

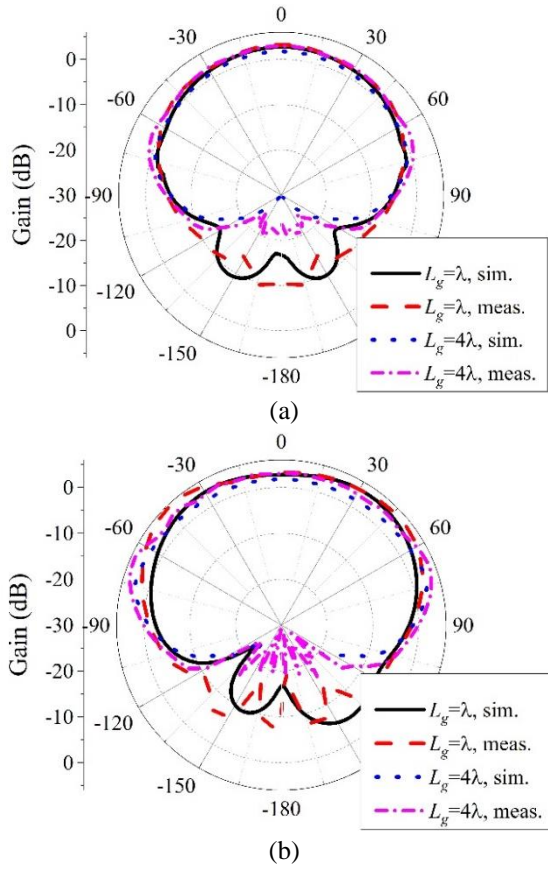


Fig. 9. Simulated and measured: (a) xz plane patterns and (b) yz plane patterns at 1.6 GHz of the hybrid-mode antenna. The 3-dB beamwidths in the xz plane and yz plane both increase with L_g .

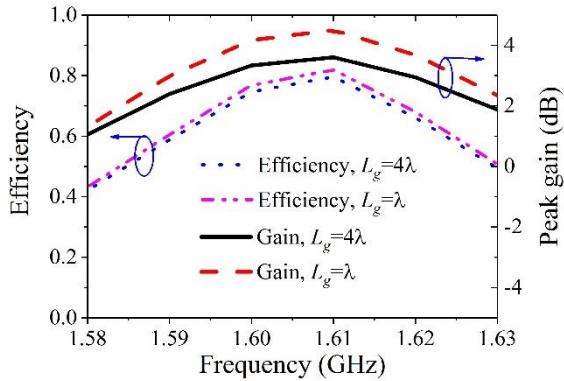


Fig. 10. Measured efficiencies and peak gains of the hybrid-mode antenna when $L_g = \lambda$ and $L_g = 4\lambda$. The peak gain in the case of $L_g = \lambda$ is a little higher than that in the case of $L_g = 4\lambda$ because the radiation beam is broader when $L_g = 4\lambda$.

III. CONCLUSION

In this paper, a low-profile hybrid-mode model is proposed to obtain a near-hemispherical coverage. Based

on this model, an on-board antenna is designed. When the side length of the ground is infinite, the 3-dB beamwidths in the xz plane and yz plane are both 180° . When the side length of the ground is finite, the proposed antenna can provide a near-hemispherical coverage. The design example demonstrates the practicability of the proposed model and the proposed antenna can be used in wide-angle scanning arrays and rich-multipath communication systems.

ACKNOWLEDGMENT

This work was supported by the National Natural Science Foundation of China (Grant Nos. 61331007, 61361166008, and 61401065), and the Research Fund for the Doctoral Program of Higher Education of China (Grant No. 20120185130001).

REFERENCES

- [1] E. E. Altshuler, "A monopole loaded with a loop antenna," *IEEE Trans. Antennas Propag.*, vol. 44, no. 6, pp. 787-791, June 1996.
- [2] E. E. Altshuler and D. S. Linden, "Design of a loaded monopole having hemispherical coverage using a genetic algorithm," *IEEE Trans. Antennas Propag.*, vol. 45, no. 1, pp. 1-4, Jan. 1997.
- [3] H. L. Sneha, S. Hema, and R. M. Jha, "Analytical estimation of radar cross section of arbitrary compact dipole array," *ACES Journal*, vol. 29, no. 9, pp. 726-734, 2014.
- [4] N. Ojaroudi, G. Noradin, and O. Yasser, "Bandwidth improvement of omni-directional monopole antenna with a modified ground plane," *ACES Journal*, vol. 29, no. 4, pp. 328-334, 2014.
- [5] P. Zibadoost, J. Nourinia, C. Ghobadi, S. Mohammadi, A. Mousazadeh, and B. Mohammadi, "Full band MIMO monopole antenna for LTE systems," *ACES Journal*, vol. 29, no. 1, pp. 54-61, 2014.
- [6] P. A. Turalchuk, D. V. Kholodnyak, and O. G. Vendik, "A novel low-profile antenna with hemispherical coverage suitable for wireless and mobile communications applications," in *Proc. IEEE LAPC*, Loughborough, UK, pp. 337-340, Mar. 2008.
- [7] P. Nayeri, A. Z. Elsherbeni, R. Hasse, and D. Kajfez, "Half-loop segmented antenna with omni-directional hemispherical coverage for wireless communications," *ACES Express Journal*, vol. 1, no. 3, pp. 88-91, Mar. 2016.
- [8] K. Nishizawa, H. Miyashita, S. Makino, and K. Sawaya, "Broadening beamwidth of E-plane radiation pattern of a dipole antenna with loaded monopole elements," in *Proc. IEEE Antennas Propag. Society Int. Symposium*, Monterey, USA, pp. 3984-3987, June 2004.
- [9] K. Nishizawa, H. Miyashita, S. Makino, and K.

- Sawaya, "Broad beamwidth and cross polarization free dipole antennas with reactive loaded monopoles," *IEEE Trans. Antennas Propag.*, vol. 55, no. 5, pp. 1230-1238, May 2007.
- [10] C. N. Hu, C. S. Chuang, D. C. Chou, and K. J. Liu, "Design of the cross-dipole antenna with near-hemispherical coverage in finite-element phased array by using genetic algorithms," in *Proc. IEEE Int. Conference Phased Array Systems Technol.*, Dana Point, USA, pp. 303-306, June 2000.
- [11] M. Scott, "A printed dipole for wide-scanning array application," in *Proc. 11th Int. Conference Antennas Propag.*, Manchester, UK, pp. 37-40, Apr. 2001.
- [12] R. Wang, B.-Z. Wang, X. Ding, Z.-S. Gong, Y. Yang, and Y.-Q. Wen, "A wide-angle scanning array based on image theory and time reversal synthesis method," in *Proc. 2015 IEEE Int. Symposium Antennas Propag.*, Vancouver, Canada, pp. 2495-2496, July 2015.
- [13] P. S. Kildal, C. Orlenius, and J. Carlsson, "OTA testing in multipath of antennas and wireless devices with MIMO and OFDM," *Proc. IEEE*, vol. 100, no. 7, pp. 2145-2157, July 2012.
- [14] A. Hussain, P. Kildal, and A. Al-Rawi, "Efficiency, correlation, and diversity gain of UWB multiport self-grounded bow-tie antenna in rich isotropic multipath environment," in *Proc. 9th Int. Workshop Antenna Technol.*, Karlsruhe, Germany, pp. 336-339, Mar. 2013.
- [15] R. Karlsson, "Theory and applications of tri-axial electromagnetic field measurements," Ph.D. dissertation, Dept. Astronomy Space Phys., Uppsala University, Uppsala, 2005.
- [16] T. D. Carozzi and G. Woan, "A generalized measurement equation and van Cittert-Zernike theorem for wide-field radio astronomical interferometry," *Monthly Notices Royal Astron. Soc.*, vol. 395, no. 3, pp. 1558-1568, May 2009.
- [17] D. S. Prinsloo, P. Meyer, R. Maaskant, and M. Ivashina, "Design of an active dual-mode antenna with near hemispherical field of view coverage," in *Proc. Int. Conference Electromagnetics Advanced App.*, Torino, Italy, pp. 1064-1067, Sep. 2013.
- [18] D. S. Prinsloo, R. Maaskant, M. V. Ivashina, and P. Meyer, "Mixed-mode sensitivity analysis of a combined differential and common mode active receiving antenna providing near-hemispherical field-of-view coverage," *IEEE Trans. Antennas Propag.*, vol. 62, no. 8, pp. 3951-3961, Aug. 2014.
- [19] Y. Li, Z. Zhang, C. Deng, and Z. Feng, "A simplified hemispherical 2-D angular space null steering approach for linearly polarization," *IEEE Antennas Wireless Propag. Lett.*, vol. 13, pp. 1628-1631, 2014.
- [20] L. Economou and R. J. Langley, "Patch antenna equivalent to simple monopole," *Electron. Lett.*, vol. 33, no. 9, pp. 727-729, Apr. 1997.
- [21] T. Kaufmann and C. Fumeaux, "Low-profile magnetic loop monopole antenna based on a square substrate-integrated cavity," *Int. Journal Antennas Propag.*, vol. 3, pp. 1-6, 2015.



Ren Wang was born in Anhui Province, China, in 1990. He received the B.S. degree in Electronic Information Science and Technology from University of Electronic Science and Technology of China (UESTC), Chengdu, in 2014. He is currently working toward the Ph.D. degree in Radio Physics at UESTC. His main research interests include time-reversed technique, compact multiport antenna, and phased array.



Bing-Zhong Wang received the Ph.D. degree in Electrical Engineering from the University of Electronic Science and Technology of China (UESTC), Chengdu, in 1988.

He joined UESTC in 1984 and is currently a Professor there. He has been a Visiting Scholar at the University of Wisconsin-Milwaukee, a Research Fellow at the City University of Hong Kong, and a Visiting Professor at the Pennsylvania State University, University Park. His current research interests are in the areas of computational electromagnetics, antenna theory and techniques, and time-reversed electromagnetics.



Xiao Ding received the B.S. and M.S. degrees in the Communication Engineering and Electromagnetic Field and Microwave Engineering, respectively, from Guilin University of Electronic Science and Technology (GUET), Guilin, China, in 2004 and 2007, respectively, and the Ph.D. degree in Radio Physics from University of Electronic Science and Technology of China (UESTC), Chengdu, China, in 2014. He joined the UESTC in 2014. In 2013, he was a Visiting Scholar at the South Dakota School of Mines and Technology, SD, USA. His research interests include short-wave, ultrashort-wave wire antennas and reconfigurable antenna and its' applications.



Changhai Hu was born in Chongqing City, China, in 1987. He received the B.S. and M.S. degrees in the Computer Science and Technology and Electromagnetic Field and Microwave Technology, from Southwest Jiaotong University (SWJTU), Chengdu, China, in 2010 and 2014, respectively. He is currently working toward

the Ph.D. degree in Radio Physics at University of Electronic Science and Technology of China (UESTC), Chengdu, China. His main research interests include ultra-wide band antenna and phased array.